Pendant-Capped Porphyrins. 2.[1] Structural Analysis and Dynamics of the Biphenyl Pendant-Capped Porphyrin Model of Catalase and Its Fe(III) Complex by One- and Two-Dimensional ^{1}H NMR Spectroscopy and Distance Geometry/Molecular Modeling Refinement

Andrei Blaskó, Barbara Garcia, and Thomas C. Bruice*

Department of Chemistry, University of California, Santa Barbara, California 93106

Received February 17, 1993 (Revised Manuscript Received May 19, 1993•)

The solution structure of a phenol pendant-capped porphyrin [(PHPCP)H_2] has been determined by two-dimensional NMR spectroscopy and Distance Geometry calculations. Sixteen internuclear distances have been obtained from rotating frame NOE (ROESY) experiments. The refined structure shows a spiral shape of the cap allowing a minimum exposure of the porphyrin core to solvent. Docking of Fe(III) into the solution structure of (PHPCP)H_2 shows that the phenolate oxygen moves 1.5 Å toward the porphyrin plane and the porphyrin ring flattens. The assignment of ^{13}C resonances for (PHPCP)H_2 (heteronuclear ^{13}C–^{1}H chemical shift correlation) and partial assignment of ^{13}C resonances for (PPCP)Fe^{III} have been done. The ^{13}C T_1 relaxation times and restrained molecular dynamics calculations for (PHPCP)H_2 show a rigid structure of the cap and a pulsing motion along the z-axis. The overall rotational coefficient was found to be 3.71×10^{-10} s. A variable temperature study of ^{1}H resonances establishes a structural change of (PHPCP)H_2 between 27–28 °C. Low-temperature study on (PHPCP)H_2 shows that the coalescence temperature of the β'/β'' pyrrole protons is −40 °C, while for the NH amide protons <−93 °C. Molecular dynamics studies on (PHPCP)H_2 and (PPCP)Fe^{III} shows a flexibility of the former and a rigidity of the latter.

Introduction

The synthesis and characterization of a phenol pendant-capped porphyrin [(PHPCP)H_2] and its iron(III) complex [(PPCP)Fe^{III}] has previously been reported.[1] The structure of the iron(III)-ligated pendant-capped porphyrin suggests an ideal model for catalase whose distal ligand is a phenolate of tyrosine. In (PPCP)Fe^{III} (a) the phenolate is positioned within bonding distance of the metal and completely isolated from outside reagents; (b) the open face allows oxidative oxygen addition to the metal; (c) the *o*-methyl substituents on the *meso*-phenyl groups at the open face prevent aggregation or μ-oxo dimer formation; and (d) the phenolate ligand is in a position to stabilize oxidation states 1e$^-$ and 2e$^-$ above the iron(III) state.

Little work has been carried out on the 3D structure of capped porphyrins, mainly because it is often difficult to obtain suitable crystals[2] for X-ray analysis. The first capped-porphyrin characterized by X-ray crystallography was the free-base porphyrin H_2-cap·5CHCl$_3$·CH$_3$OH (H_2-Cap).[2] Later the X-ray structural characterization of two novel four-atom-linked capped porphyrins (4-Cap)[3] was accomplished and recently, the X-ray structure of Fe(C_2-Cap)(CO)(1-MeIm), in which the free base is H_2-Cap {in ref 3 described as H_2(C_2-Cap)}, has been determined.[4] The attempt to obtain X-ray quality crystals of (PHPCP)H_2 failed.

One of the most powerful tools for structural analysis of relatively complex organic molecules is two-dimensional (2D) NMR spectroscopy which provides a complementary method for X-ray crystallography. The solution structure of a bicyclo[2.2.2]octane-Cap(ped) porphyrin has been determined by 2D ^{1}H NMR.[5] A convenient way to study dynamic properties in solution is by quantifying the segmental motions in the molecule using ^{13}C spin-lattice relaxation times (T_1). ^{13}C T_1's in tetraphenyl porphyrins are generally short (ca. 1 s)[6] and are mainly dominated by a dipolar mechanism. By lowering the temperature, the porphyrin molecule slows down its motion and the ^{13}C T_1 values decrease rapidly.[7] Variation in the total energy of the porphyrin due to the temperature change can lead to conformational changes.

Our goal was to determine the solution structure of (PHPCP)H_2 and its Fe(III) complex using rotating frame NOE experiments (ROESY) and Distance Geometry (DGEOM) calculations for the refinement of the NMR structural data. Also described is the dynamic behavior of (PHPCP)H_2 and the structural changes which occur with temperature change. The structure of (PPCP)Fe^{III} was approximated by CHARMm energy minimization.

RESULTS

ROESY calculations. ROESY spectra for (PHPCP)H_2 were recorded at a mixing time τ_m, of 50 and 200 ms. The data at τ_m = 50 ms exhibit small ROESY enhancements ruling out quantitative analysis. Previous studies on bicyclo[2.2.2]octane-Cap porphyrin showed linearity in the 50–200 ms mixing-time domain.[5] The structural and conformational analysis of (PHPCP)H_2 in CDCl$_3$ solution was achieved by quantifying the ROESY

• Abstract published in *Advance ACS Abstracts,* September 1, 1993.

[1] The first paper in the series is "The Synthesis of a Biphenyl Pendant-Capped Iron(III) Porphyrin Model of Catalase", Garcia, B.; Lee, C.-H.; Blaskó, A.; Bruice, T. C. *J. Am. Chem. Soc.* **1991**, *113*, 8118.

[2] Jameson, G. B.; Ibers J. A. *J. Am. Chem. Soc.* **1980**, *102*, 2823.

[3] Johnson, M. R.; Seok, W. K.; Ibers, J. A. *J. Am. Chem. Soc.* **1991**, *113*, 3998.

[4] Kim, K.; Ibers, J. A. *J. Am. Chem. Soc.* **1991**, *113*, 6077.

[5] Zang, H.-Y.; Blaskó, A.; Yu, J.-Q.; Bruice, T. C. *J. Am. Chem. Soc.* **1992**, *114*, 6621.

[6] Huet, J.; Gaudemer, A. *Org. Magn. Reson.* **1981**, *15*, 347.

[7] Stilbs, P. *J. Magn. Reson.* **1984**, *58*, 152.

0022-3263/93/1958-5738$04.00/0

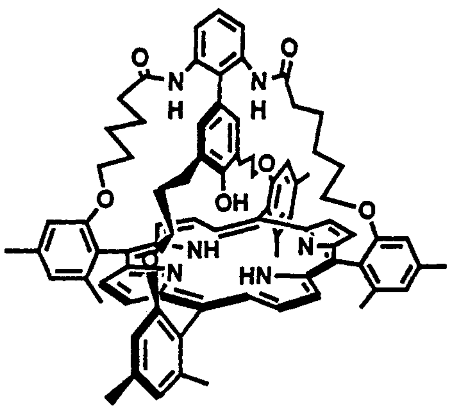

$(PHPCP)H_2$

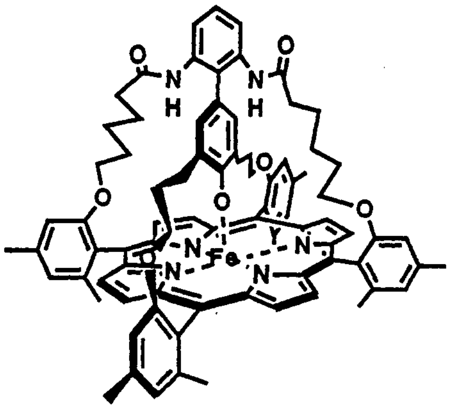

$(PPCP)Fe^{III}$

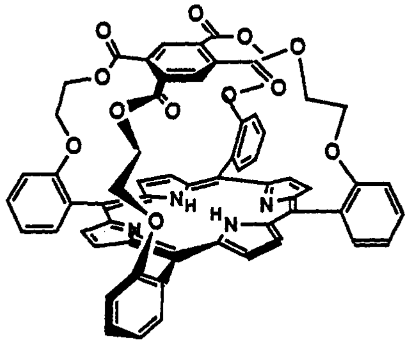

H_2-cap

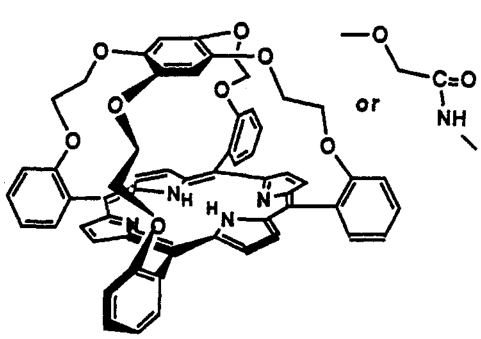

4-Cap

experimental data at a mixing time, τ_m,of 200 ms. An expanded contour plot of the ROESY spectrum is shown in Figure 1. Assuming that proton–proton interactions can be described by the same correlation time, the ROESY peaks can be related to the 6th power of the distance between protons involved in interactions[8] (Experimental Section, eq 4). Average distances were calculated for 12 interactions (Chart I), taking the separation of H3′ and H4′ of the phenyl ring to be that (2.46 Å) obtained by energy minimization of $(PHPCP)H_2$.[9] Although the capping of the porphyrin brings a fairly rigid structure, the existance of five methylenes on the A(B) leg (Chart I) allows some flexibility and certain conformational changes with interacting solvents. ROESY peaks were seen between H2,6 of the pendant phenyl ring and the β methylene protons of the A(B) leg and between the ϵ methylene of the A(B) leg and the E protons of the *meso*-phenyl substituents (Figure 1 and Table I). On the C(D) leg, the c protons interact with the E′ *meso*-phenyl protons. These through-space interactions will define the geometry of the legs and were used in the structural calculations. The ROESY distances and their refined values for the most stable conformer (no. 86, E = 76.0 kcal/mol) are shown in Table I.

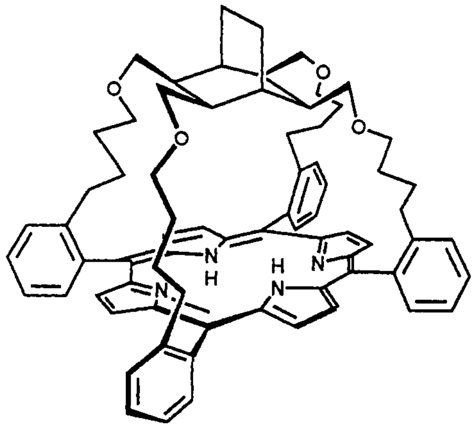

bicyclo[2.2.2]octane-Cap

Distance Geometry (DGEOM) Calculations. An initial structure of $(PHPCP)H_2$ was constructed using the computer program QUANTA and its energy was minimized in CHARMm (Polygen Corp.[9]). The coordinates of this minimized structure of $(PHPCP)H_2$ were entered into the DGEOM program[10] along with the 12 distance constraints (Experimental Section) derived from the ROESY data (Table I, marked with asterisk). The upper bond distances were set 10–15% higher than the NMR distances while the lower bond distances were allowed to equal the van der Waals distance separations. We did not include the α–γ and b–a distance constraints because they belong to the same chain and could be affected by spin

---

[8] (a) Kessler, H.; Bats, J. W.; Griesinger, C.; Koll, S.; Will, M.; Wagner, K. *J Am. Chem. Soc.* **1988**, *110*, 1033. (b) Kessler, H.; Griesinger, C.; Kerssebaum, R.; Wagner, E.; Ernst, R. *J Am. Chem. Soc.* **1987**, *109*, 607.

[9] Quanta, version 3.2.3; CHARMm, version 21.3 Polygen Corp., Waltham, MA, 1991. See Brooks, B. R.; Bruccoleri, R. E.; Olafson, B. D.; States, D. J.; Swaminathan, S.; Karplus, M. *J. Comput. Chem.* **1983**, *4*, 187.

[10] Blaney, J. M.; Crippen, G. M.; Dearing, A.; Dixon, J. S. E. I. du Pont de Nemours & Co., 1990.

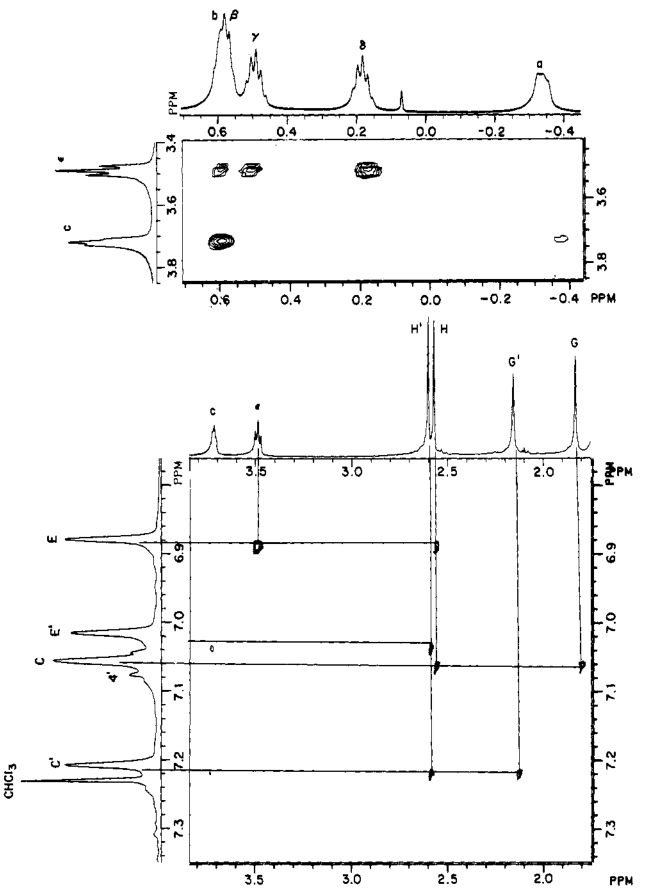

Figure 1. Expansions of the ROESY spectrum of (PHPCP)H_2 0.01 M in $CDCl_3$ at 25 °C (500 MHz) with a mixing time of 200 ms and a spin locking field strength of 2.5 kHz.

Chart I

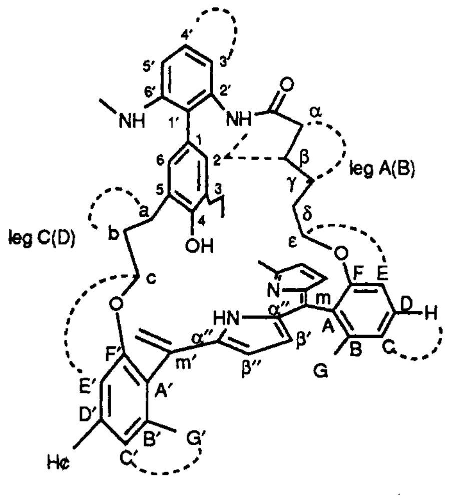

diffusion. Also we did not include NH-2,6 because the NOE buildup is restricted by the dynamics of the amide bond (*vide infra*).

One hundred conformers of (PHPCP)H_2,which fit the ROESY constraints, were generated by use of the DGEOM program. By use of the DGEOM subprogram COMPARE there was generated a symmetric 100 × 100 matrix of least-squares rotation/translation fit root mean square (RMS) errors. The RMS matrix was subjected to a cluster analysis[11] which allowed the choice of grouping the 100 conformers into 20 conformational "families" using the statistical program Data Desk.[10] One representative conformer was chosen from each "family" and energy minimized. The spread in energy content for the 20 minimized conformers is about 32 kcal/mol (Table S1). The most stable conformer with E = 76.0 kcal/mol (Table S1, no. 86 and Figure 2a) was mapped and the core size was defined (Table II and Experimental Section).

Table I. Experimental and Calculated Distances for (PHPCP)H_2 (Å)

		calculation[b]			
H–H	exp[a]	leg A	leg B	leg C	leg D
E′–c*	2.89	–	–	2.88	2.97
E–ε*	2.61	2.11	2.22	–	–
3′–4′	2.46[c]	2.45	2.47	–	–
C–H	2.67	2.47	2.48	–	–
C′–G′	2.85	–	–	2.48	2.49
2,6–β*	3.03–3.06	2.93	3.66	–	–
NH–2,6	5.96	2.16	2.83	–	–
α–γ	3.35	2.56	2.53	–	–
b–a	3.05	–	–	2.60	2.52

[a] From ROESY data (25 °C, $CDCl_3$). [b] From the most stable conformer using as distance constraints the interactions marked with an asterisk. [c] Distance from energy minimization and as a standard.

It was found that the total energy of the minimized conformers arose primarily from electrostatic and van der Waals contributions (Table S1). The refined distance values for the most stable minimized DGEOM conformer is consistent with the NMR data (Table I). The differences between the calculated H-H distances and those determined from ROESY data for legs A and B come from the position of the phenyl dome which has a slight lateral shift, Δ (Chart II), with respect to the porphyrin plane of 1.2 Å as it was seen in the case of other substituted porphyrins.[12] There is also a rotation of the cap with respect to the porphyrin ring of 29.5° which leads to a spiral shape of the connecting legs. These two features, the lateral shift and the rotation of the cap, define the relative positions of the methylene protons of the four legs.

The shortest H-H distance has the major contribution to the ROESY peaks buildup because the signal decreases with the 6th power of the H-H distance (eq 4, Experimental Section). The three dimensional structure (Figures 2a and 7g) of (PHPCP)H_2 determined by these techniques show a rotation + translation of the cap, corresponding to a helical turn of 3.0° per each angstroms which separates the porphyrin ring from the cap (Experimental Section).

This feature allows (PHPCP)H_2 ($CDCl_3$ solution) to assume a compact structure due to the screwing down of the cap. The difference in the dihedral angles for the two amide groups (legs A and B, respectively), 6.6° and 166.0° for (PHPCP)H_2 and 30.9° and 164.8° for (PPCP)Fe^{III}, relate to the sigmoidal shape of the connecting legs. We saw only one $\beta'\beta''$ (pyrrole) and one NH (amide) as sharp signals at 25 °C in $CDCl_3$, but three (two separated and two overlapped) $\beta'\beta''$ signals and broadening of the NH (amide) signal at −93 °C (CD_2Cl_2) (*vide infra*). The structural characteristics of (PHPCP)H_2 and (PPCP)Fe^{III} are summerized in Table II.

A referee suggested that our determined solution structure of (PHPCP)H_2 was actually created by the procedures of DGEOM, Data Desk, and molecular mechanics minimizations and that the ROESY constraints do not influence the structure. When the procedures of

---

(11) Data Desk, version 3.0, Odesta Corp., Northbrook, IL, 1989.

(12) Seungwon, J.; Almarson, Ö.; Rafik K.; Blaskó, A.; Bruice, T. C. *Inorg. Chem.* 1993, *32*, 2562.

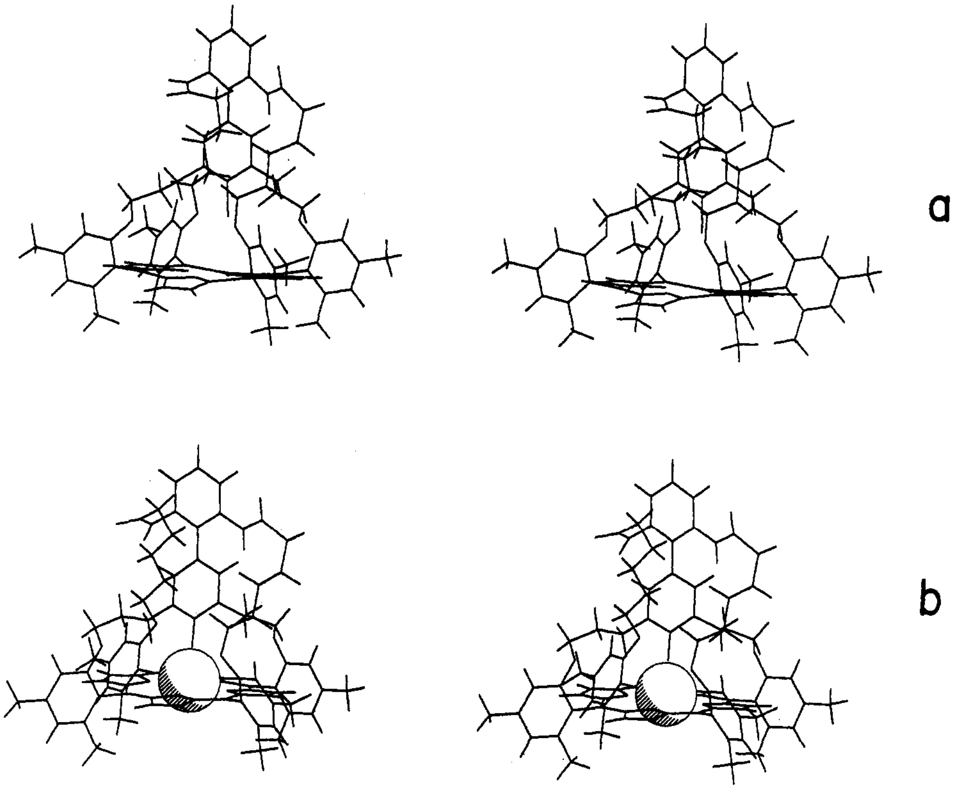

Figure 2. Stereo models of (a) (PHPCP)H_2 and (b) (PPCP)Fe^{III}. The iron atom is shown as a CPK model. The porphyrin ring flattens upon the Fe(III) insertion and the core size decreases. Due to the view angle some of the CH_2 protons are obscured; see also Figure 9b.

Table II. Structural characteristics for (PHPCP)H_2 and (PPCP)Fe^{III}

structural parameters	(PHPCP)H_2	(PPCP)Fe^{III}
lateral shift (Å)	1.2	0.6
core height[a] (Å)	3.52	2.01
helical turn for A and B (deg/Å)	3.03	3.78
dihedral angle (deg) amide A	6.64	30.09
amide B	-166.0	-164.8
tilt of pyrroles (deg) leg A/B[b]	0.60/0.48	1.79/0.93
leg C/D	2.21/6.19	2.75/0.35
Σ tilt	9.48	5.82
twist of pyrroles (deg) leg A–B	-1.34	-6.4
leg C–D	0.76	-6.4

[a] As the distance between the phenolic oxygen and the center of the porphyrin ring. [b] The pyrrole on the right side of each leg was labeled with the name of the leg.

DGEOM, Data Desk, and molecular mechanics minimizations were applied without ROESY constraints we obtained a structure in which the experimental ϵ–E distance constraints were not met, and the legs A and B were not symmetrical (Figure S3). According to this derived structure, the ϵ protons of leg A would have a highly shielded position but the ϵ protons of leg B would not. However, we find that the ϵ protons of legs A and B have the same chemical shift (Figure 1). Thus, inclusion of ROESY constraints in DGEOM and molecular mechanics minimization provides a most stable structure with experimentally determined ROESY distances.

The Cavity Size for (PHPCP)H_2 and (PPCP)Fe^{III}. The free space under the cap can be visualized with the use of "brick maps" (Figure 3) showing the volume within the van der Waals radii separation. Examination of conformers shows that the sizes of cavities of the conformers increase with increasing total energy (Figure 3).

Chart II

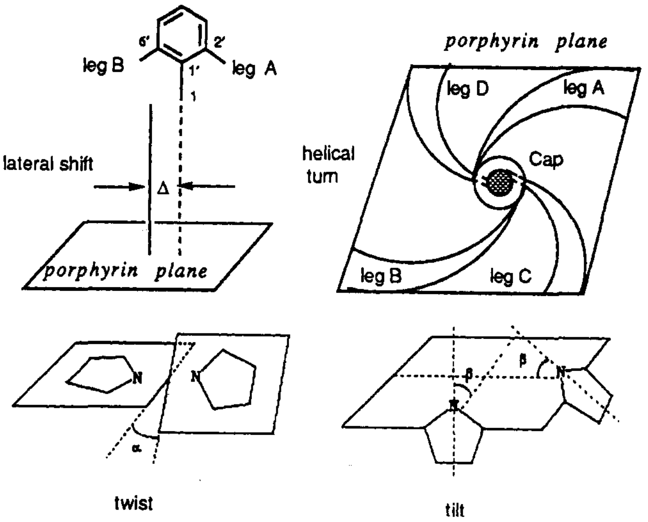

The most probable (PHPCP)H_2 solution structure was used to obtain the (PPCP)Fe^{III} structure by docking an Fe(III) inside its cavity. The structure obtained was minimized in CHARMm with ABNR parameters (Experimental Section). With the Fe(III) ligated to the phenoxide oxygen and the pyrrole nitrogens, any other interactions under the cap are forbidden. The distance between the phenolic oxygen and the center of the porphyrin plane decreases from 3.52 to 2.01 Å and the porphyrin ring flattens (Table II and Figure 2). The ruffling of the porphyrin ring was characterized by the twist (α) and the tilt (β) of the pyrroles. Their average values decrease as the Fe(III) complex is formed (Table II).

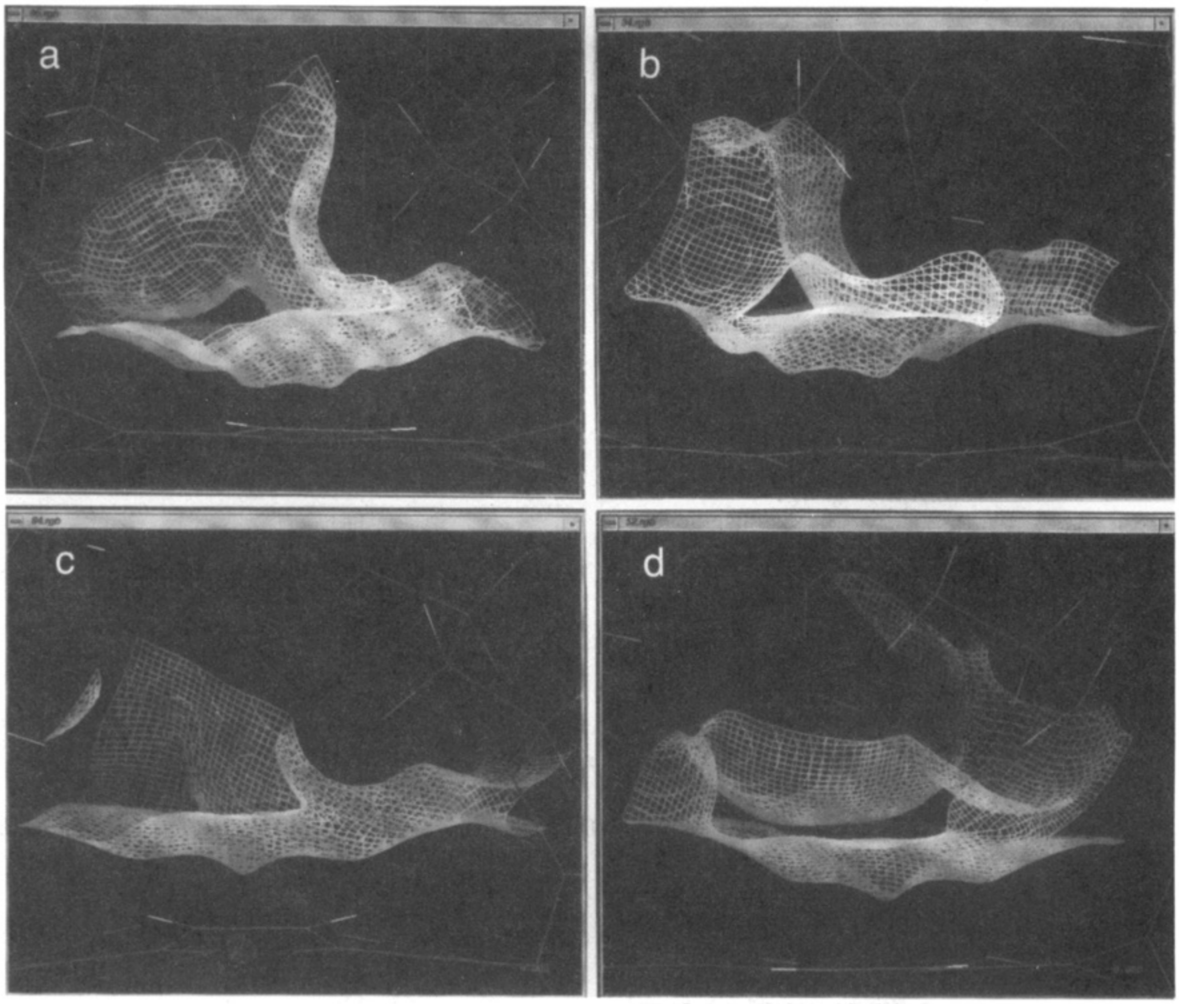

Figure 3. Brick maps of structures: (a) no. 86 (E = 76 kcal/mol), (b) no. 34 (E = 85 kcal/mol), (c) no. 84 (E = 96 kcal/mol), and (d) no. 52 (E = 108 kcal/mol) for (PHPCP)H_2, showing the porphyrin core at the van der Waals radii surface. The core size increases with the energy increase and the porphyrin distorts.

^{13}C Experiments. ^{13}C Spin-Lattice Relaxation Times (T_1) and Molecular Dynamics. Assignment of ^{13}C chemical shifts for (PHPCP)H_2, based on 1D ^{13}C NMR and the Attached Proton Test (APT) experiment has been reported.[1] The 2D ^{13}C–^1H chemical shift correlation (Figures 4, S1, and S2) confirms most of the ^{13}C resonances. However, for some very close resonances we found inversions, such as C(C′)–2(6), E–E′, ϵ–c, γ–β and H(H′)-G(G′) (Table III and ref 1).

The ^{13}C NMR spectrum of the high-spin (s = 5/2) (PPCP)Fe^{III} shows high-field resonances that are typical for paramagnetic iron porphyrins (Figure 5). On the basis of a comparison with the ^{13}C NMR spectrum reported for the related *meso*-(5,10,15,20-tetraphenylporphinato)iron chloride,[13] the resonances at 445 and 415 ppm (line width, 7500 Hz; 25 °C) have been assigned to the β''- and β'-carbons and the resonances at 337 and 328 ppm (line width, 800 Hz; 25 °C) have been assigned to the *meso*-carbons (m′ and m). The peak at 461 ppm (line width, 2500 Hz; 25 °C) probably arises from 4 due to its close proximity to the paramagnetic Fe(III). The resonances at −33 and −37 ppm have been assigned to the A and A′.

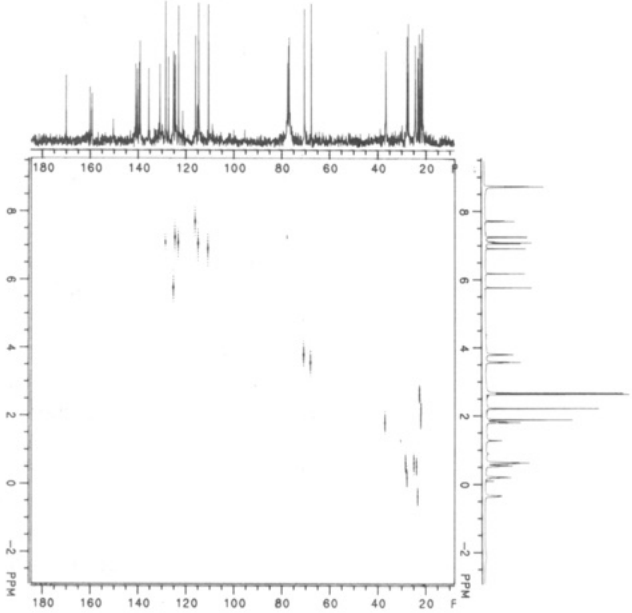

Figure 4. ^{13}C–^1H chemical shift correlation of (PHPCP)H_2 at 25 °C in $CDCl_3$. The ^1H resonances were previously assigned (DQF-COSY).[1]

There is little work on ^{13}C T_1 of substituted tetraphenyl porphyrins and their metallocomplexes.[6,12,14] The ^{13}C spin-lattice relaxation times for free-base porphyrins are

---

[13] (a) Goff, H. *Biochim. Biophys. Acta* **1978**, *542*, 348. (b) Mispelter, J.; Momenteau, M.; Lhoste, J.-M. *J. Chem. Soc. Dalton Trans.* **1981**, *8*, 1729.

Table III. ^{13}C Chemical Shifts and T_1 Relaxation Times for $(PHPCP)H_2$ in $CDCl_3$ at 125.76 MHz and 25 °C[a]

carbon	δ (ppm)	T_1 (s)	carbon	δ (ppm)	T_1 (s)
G,G′	21.29	0.77	C	122.93	0.21
H,H′	21.96	0.76	C′	124.38	0.19
a	22.62	0.26	2,6	125.04	0.20
γ	23.17	0.20	A,A′	127.17	1.08
β	24.23	0.19	4′	128.35	0.55
δ	27.16	0.19	β′,β″	130	0.18
b	27.66	0.22	3,5	130.72	0.67
α	36.35	0.20	2′,6′	135.42	1.13
ϵ	67.52	0.16	D	139.05	0.83
c	70.35	0.20	D′	139.28	0.76
E	110.43	0.21[b]	B	140.11	0.98
E′	114.50	0.21[b]	B′	140.80	0.90
m	114.54	0.50	4	150.23	1.72
m′	115.17	1.70	F	159.06	1.48
3′,5′	115.90	0.18	F′	159.89	1.70
1′	121.29	0.75	C=O	169.89	1.51
1	122.45	0.74			

[a] Values are not corrected for the different numbers of protons attached (see text). [b] E,E′ measured together. Note the values of T_1: a > α, b > β, c > ϵ.

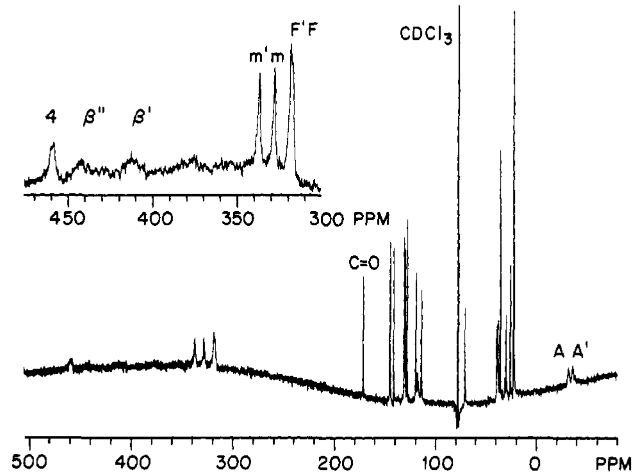

Figure 5. ^{13}C NMR of $(PPCP)Fe^{III}$, 10 mM in $CDCl_3$ at 25 °C.

typically dominated by dipole–dipole interactions and the T_1 values can be related to an average correlation time τ_c.[15,16] For a molecule rotating isotropically, the correlation time τ_c is a function of the correlation time for the overall reorientation of the molecule, τ_r, and an effective correlation time for the internal motion, τ_i[15] (eq 1). For

$$1/\tau_c = 1/\tau_r + 1/\tau_i \tag{1}$$

molecules with fast overall reorientation, τ_r dominates τ_c. As molecular size and solvation increase, the overall reorientation becomes slower; τ_i then becomes more important and eventually dominates τ_c. In the case of meso-substituted tetraphenyl porphyrins and their metal complexes,[17] τ_c is 1.0–1.5 × 10^{-10} s, which corresponds to an overall rotational diffusion coefficient, D_o = 1.1–1.7 × 10^9 s^{-1}, and is defined by the Stokes–Einstein–Debye equation (eq 2),[15,17] where η is the viscosity, k the

$$\tau_c = (4\pi/3)(a^3\eta/kT) = 1/6D_o \tag{2}$$

Boltzmann constant, and a is an equivalent radius of the molecule. The contribution of the intramolecular diffusion coefficient D_i to τ_c is small, therefore τ_c will be still dominated by τ_r. The capping of the porphyrin makes τ_i negligible in the τ_c expression and the contribution of other mechanisms to the relaxation times can also be neglected.[6] The relaxation time, T_1, of a carbon nucleus is related to the effective correlation time τ_c, which characterizes the rate of reorientation of the relaxation vector ^{13}C–^1H (eq 3).[15] In eq 3, N_H is the number of protons directly bounded

$$\frac{1}{T_1} = \frac{0.66 N_H\, \gamma_H^2 \gamma_C^2 \hbar^2}{r_{C\text{-}H}^6} \times \tau_c \tag{3}$$

to the carbon atom; $\hbar = h/2\pi$, Planck's constant; γ_H, γ_C, gyromagnetic ratios for ^1H and ^{13}C; and $r_{C\text{-}H}$, the C–H bond length. The T_1 values for the protonated $(PHPCP)H_2$ carbon atoms are in the range of 0.1–0.8 s (Table III). If we consider an isotropic motion of the molecule, its overall tumbling can be described by the effective correlation time of the monoprotonated carbons attached to a rigid part of the molecule (β′,β″,3′,5′). An average T_1 of about 0.18 s for the ^{13}C β′,β″ and 3′,5′ atoms corresponds to an overall rotational diffusion coefficient, D_o, of 4.5 × 10^8 s^{-1}. The T_1 relaxation time for the A(B) leg increases from ϵ to β and decreases again at the α carbon (Table III). On the C(D) leg, there is an increase from carbon c to carbon a. The T_1's are slightly higher for the C(D) leg. The quaternary *meso*-carbons, m and m′, have different T_1 values, although these values cannot be compared with the protonated carbon T_1's. The m′ carbon has three times smaller T_1 than the m carbon. The methyl G,G′, H,H′ carbons have T_1's of about 0.77 s (Table III), which can be compared to the methylene carbons of the legs, in a crude aproximation, by multiplying this value by $^2/_3$, accounting for the number of attached protons,[16] although the T_1's of the methyl carbon nuclei are usually much longer than permitted by the ratios $\{T_1(CH)/T_1(CH_2)/T_1(CH_3) = 6:3:2\}$[16] expected for the dipole–dipole mechanism.

Variable Temperature Study. Variable temperature (VT) studies were performed in $CDCl_3$ (5–55 °C) and CD_2Cl_2 (−93–10 °C). In $CDCl_3$, $(PHPCP)H_2$ shows a break in the ^1H chemical shift profiles (Figure 6) which occurs between 20 and 30 °C. This is clearly seen in the case of the γ, δ, a and bβ ^1H resonances (note that b and β signals are overlapping). Similar behavior is exhibited by β′(β″), c, and the amide resonances. This is mainly due to the shielding and deshielding effects of the aromatic ring and, as the legs' protons interact with the pendant phenol and the porphyrin aromatic rings, they will not shift only monotonically, but also will give a break in the plot. No major break can be seen on the other VT dependencies, although it is noticeable. The ^1H VT plot for α, C′, and HH′ does not show any changes between 5 and 55 °C (Table S2) and therefore they do not change their positions. By examining the chemical shift changes of the γ and δ resonances, one can clearly see that at 27–28 °C there is a net change of the $(PHPCP)H_2$ conformation.

---

(14) (a) Kabbani, A. T.; La Mar, G. N. *J. Magn. Reson.* **1981**, *43*, 90. (b) Yamamoto, Y.; Nanai, N.; Chujo, R.; Inoue, Y. *Bull. Chem. Soc. Jpn.* **1991**, *64*, 3199. (c) Rafik, K.; Almarson, Ö.; Blaskó, A.; Bruice, T. C. *J. Org. Chem.*, **1992**, *57*, 1269.

(15) Lyera, J. R.; Levy, G. C. In *Topics in Carbon-13 NMR Spectroscopy*; Levy, G. C., Ed.; John Wiley: New York, 1974; Vol. 1, Chapt. 3.

(16) Breitmaier, E.; Voelter, W. *Carbon-13 NMR Spectroscopy*, 3rd ed., VCH Publ.: New York, 1987, p 163.

(17) Cassidey, L.; Bang, H.; Edwards, J. O.; Lawler, R. G. *J. Phys. Chem.* **1991**, *95*, 7186.

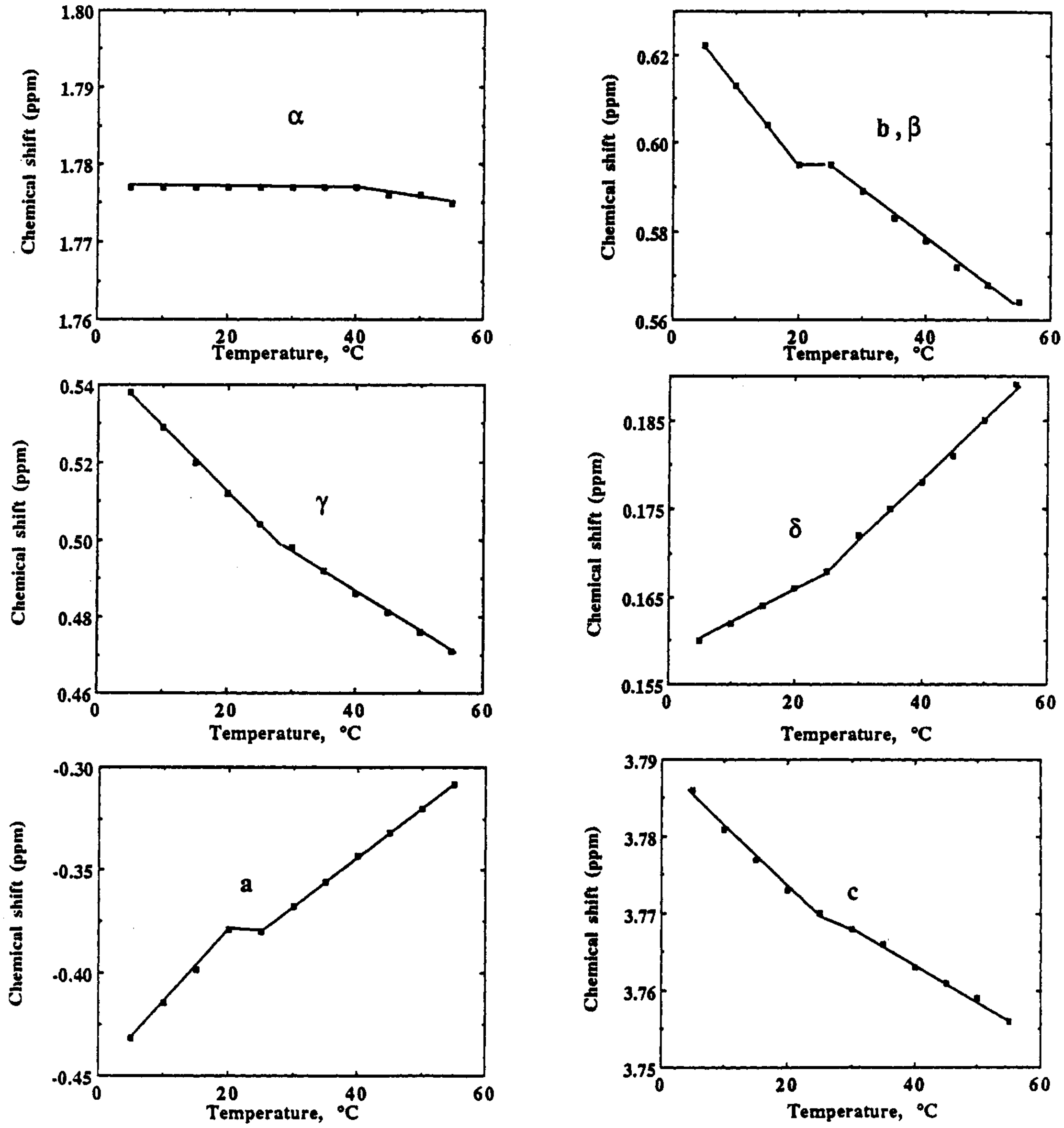

Figure 6. ^1H chemical shift temperature dependence for $(PHPCP)H_2$ for the selected protons.

In order to test the nonequivalency of the $\beta'\beta''$ (pyrrole) and NH (amide) protons, a low temperature study was performed in CD_2Cl_2 (Figure 7). The $\beta'\beta''$ signals start to broaden at −10 °C and we saw two signals at 8.63 and 8.76 ppm, respectively, at −40 °C. Both signals sharpen between −40 and −80 °C. The signal at 8.63 ppm starts to broaden again at −80 °C and is resolved into two new signals at −90 °C (8.64 and 8.66 ppm) with a slight temperature shift. The signal at 8.76 ppm sharpens when going from −40 to −90 °C. No differences were seen at −90 and −93 °C in the $\beta'\beta''$ line widths. The NH (amide) signal at 6.16 ppm (CD_2Cl_2) maintains its line width, $\nu_{1/2}$, of 5 Hz when going from 10 to −70 °C. At −80 °C the NH (amide) signal broadens to 7 Hz and at −93 °C to 9 Hz. The chemical shift difference of the NH (amide) resonance between −10 and −93 °C was 0.06 ppm. We also noticed two sets of methylene resonances at −40 °C (coalescence temperature −30 °C) and sharpening of the NH (pyrrole) resonance (−2.6 ppm) with the temperature decrease.

Molecular dynamics calculations have been performed (30 ps) on $(PHPCP)H_2$ and $(PPCP)Fe^{III}$. Restrained molecular dynamics calculations were performed on **$(PHPCP)H_2$** at 25 °C starting with the refined DGEOM structure with ROESY constraints. The torsion angles of the amide bonds for legs A and B have a spread of 100° and 140° for the *trans*(*Z*) and *cis*(*E*) conformers, respec-

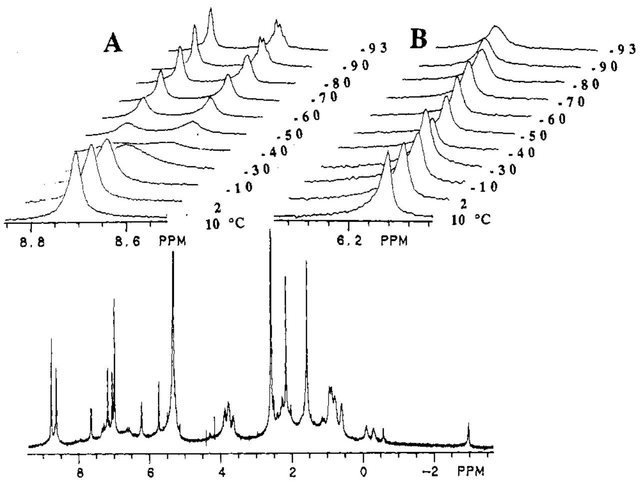

Figure 7. ^1H NMR of $(PHPCP)H_2$ at −93 °C in CD_2Cl_2. Inset (A) Stacked plot of the aromatic region and (B) the NH (amide) region at the indicated temperatures.

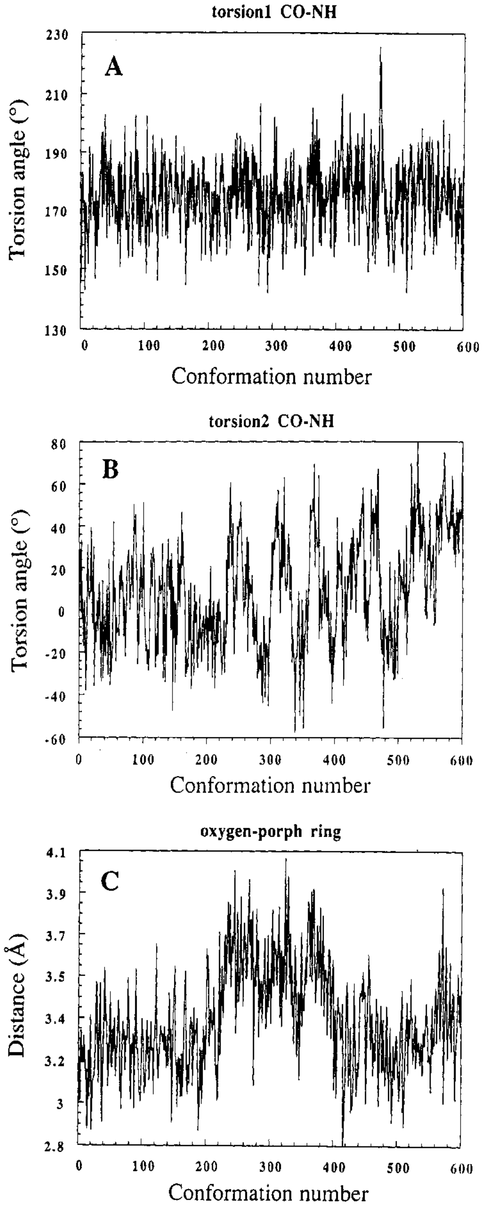

Figure 8. Trace plots (30 ps) for the amide torsion angles (A, B) and for the phenol oxygen center of the porphyrin ring distance (C).

tively (Figure 8A,B). The distance between the phenol oxygen of the pendant cap and the center of the porphyrin ring ranges between 2.8 and 4.1 Å (Figure 8C). The distance ranges between carbons γ (leg A), γ (leg B), b (leg C), and b (leg D), as centers of the methylene chains, are 6.8–8.3, 7.2–8.4, 4.3–6.7, and 4.2–6.5 Å, respectively.

In order to compare the flexibility/rigidity of (PHPCP)H_2 and (PPCP)Fe^{III} a molecular dynamics study without constraints was performed on both molecules at 55 °C because the motion is larger than at 25 °C. As a measure of the segmental mobilities, the distances between the opposite γ (legs A and B) and the opposite b (legs C and D) carbons were chosen. It was found that the maximum distance changes between the γ carbons of legs A and B is 1.2 and 1.3 Å for (PHPCP)H_2 and (PPCP)Fe^{III}, respectively, while for the b carbons of legs C and D they are 1.4 and 0.8 Å.

Discussion

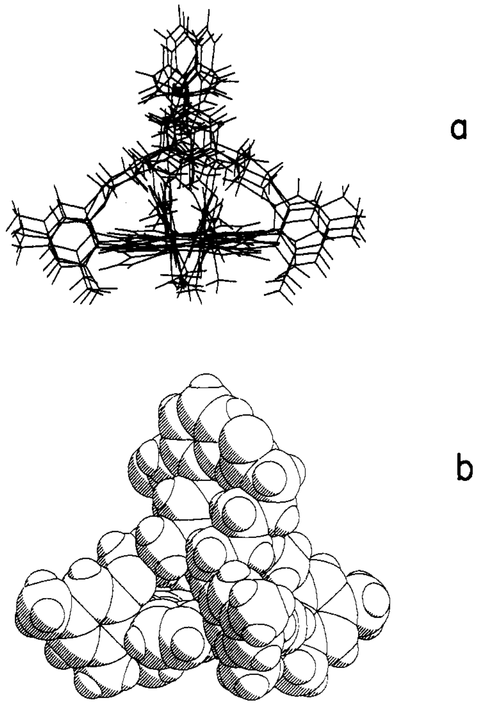

Figure 9. (a) Overlay of four structures of (PHPCP)H_2 (no. 86, no. 34, no. 84 and no. 52) with different energies obtained fron DGEOM calculations and CHARMm minimized. (b) CPK model

The capping of a tetraphenyl porphyrin (TPP) brings new features to the TPP molecule. We describe the solution 3D structure and dynamics of a pendant-capped porphyrin (PHPCP)H_2 and propose the structure of its Fe(III) complex (PPCP)Fe^{III}. *Ortho* substituents on the *meso*-phenyls of (PPCP)Fe^{III} will forbid the formation of μ-oxo dimers, while the cap will allow just one open face for electron transfer and ligation. As a model for catalase, the phenolate substituent must ligate to Fe(III) in order to stabilize intermediate hypervalent iron-oxo species. The structure of (PHPCP)H_2 shows two interesting characteristics: ruffling of the porphyrin ring and a spiral shape of the cap as seen in the case of other capped-porphyrins.[17,12] The solution structure of (PHPCP)H_2, determined by ROESY–DGEOM calculations allows a minimum exposure of the porphyrin to the solvent molecules by ruffling of the porphyrin ring and down screwing of the pendant cap (Figures 2a and 9b). The distance constraints play an important role in the structural determination of (PHPCP)H_2 and confer a spiral shape to the capping structure. However, this structure has to be regarded as a dynamic entity as the ^{13}C T_1 relaxation times (Table III) and restrained molecular dynamics establish (Figure 8). The differences in the ^{13}C T_1 relaxation times for the methylene carbons of (PHPCP)H_2 indicate that the motion of the cap occurs in a way that the methylene carbons of the C(D) leg are more mobile than the methylene carbons on leg A(B). The differences in the T_1 values (Table III) for the two methylene segments of legs A(B) and C(D) (<0.1 s) raise the question of the accuracy of the method. It is known that T_1 values have a margin of errors of up to 20%.[15,16] Although the differences are small, we find T_1 {leg A(B)} < T_1 {leg C(D)}. The segmental motion of the four legs causes difficulties in the NOE buildup for the 2,6-NH resonances; therefore the experimental NOE distance in this case does not reflect reality. It is consistent though with the conclusions from the T_1 (Table III) and molecular dynamics analysis (Chart III and Figure 8, *vide infra*) of (PHPCP)H_2.

Chart III

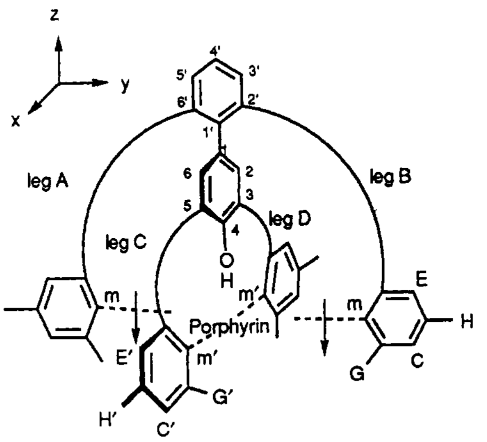

The two amide bonds of the capping structure actually exist in a cyclic structure such that one existing in *cis*(E) form should not be surprising. Cyclic peptides can have energetically favorable *cis*(E) conformations.[18] The existence of only one NH (amide) resonance at 25 °C must be explained. Molecular dynamics simulations provide the best evidence for the mobility of the amide bonds. The molecular dynamics study on (PHPCP)H_2 (30 ps) shows that the torsion angle span for the *trans*(Z) and *cis*(E) conformations of the amide bonds is 100 and 140°, respectively (Figure 8A,B). These motions would insure a single amide resonance at 25 °C. Much above −80 °C there is only one NH (amide) signal but by −80 °C this signal has begun to broaden as if approaching the coalescence temperature where *cis*(E) and *trans*(Z) forms can be differentiated. The two amides in (PHPCP)H_2 have different dihedral angles between the CO and NH groups in the lowest energy structure. While the *trans*(Z) form is common for unsubstituted amide groups, *cis*(E) forms are frequently encountered in N-substituted peptides.[18] In reality, rigid planar *cis* or *trans* conformations do not exist in many peptide molecules. The separation of the $\beta'\beta''$ (pyrrole) signals at −40 °C shows that the porphyrin ring will be the first to decrease its mobility, while the amides the last.

By molecular dynamics, the translation about the z-axis (Chart III), described by the distance span between the phenol oxygen and the center of the porphyrin ring of 1.3 Å (Figure 8C), is associated with a rotation of the cap. As expected, this motion is associated with the ruffling of the porphyrin ring. This ruffling is consistent with the different T_1 values for the *meso*-carbons (m, m′) indicating a rigidity of the m′(leg C)–4–m′(leg D) arch as compared to the m(leg A)–1′–m(leg B) one. Therefore, the ruffling of the porphyrin ring must occur symmetrically to the m′(leg C)–m′(leg D) axis shown by arrows in Chart III. The pulsing of the molecule about the z-axis and the ruffling of the porphyrin ring should affect the tetraphenyl substituents also. The peripheral position in this context requires quite large and similar values for G(G′), H(H′) and C(C′), E(E′). A modification only of the dihedral angle of the phenyl substituents with respect to the porphyrin ring (FAmα' and F′A′m′α'', Chart I) would give different T_1 values for H(H′) and G(G′), since this motion will occur about the H(H′)–m(m′) axis of the phenyl ring (Chart III). This is not the case (Table II) and the motion is that shown by the arrows in Chart III as discussed above. Low temperature study on (PHPCP)H_2 shows that the molecule slows down its motion starting with the porphyrin ring and ending with the capping structure. The conformational change at around 27–28 °C, monitored by the γ and δ resonances, relates to the formation of a screwed-down structure of (PHPCP)H_2 when lowering the temperature. When monitoring b,β and c, the VT plot profile changes between 20–25 °C relate to their stereochemistry and proximities to the pendant phenol and porphyrin core. Those structures of (PHPCP)H_2 with higher energies than 76 kcal/mol will allow changes in the methylenes' position with respect to the pendant phenyl ring. Some of them will change from a deshielded to a shielded position {δ, a, NH_{pyrr}, NH_{amide}, 3′(5′)}, some of them from a shielded to a deshielded position (γ, b, β), while others will maintain their initial positions {(α, C′, H, H′), Figure 6 and Table S2}. This can also be related to a break of the phenolic OH hydrogen bonding to the pyrrole nitrogens of the porphyrin core. The molecular dynamics calculations show that (PPCP)Fe^{III} is more rigid, rigidity brought by the Fe(III) ligation. There is a decrease in segmental mobilities for legs C and D in (PPCP)Fe^{III} as compared to (PHPCP)H_2.

Conclusions

Structural analysis of **(PHPCP)H_2** and **(PPCP)Fe^{III}** has been accomplished by one- and two-dimensional ^1H NMR spectroscopies and Distance Geometry calculations (molecular mechanics refinement). The ROESY data on (PHPCP)H_2 allowed us to input NOE constraints into the DGEOM program and, by a cluster analysis followed by CHARMm minimizations, to determine the most probable solution structure of (PHPCP)H_2. This is the only structure available in the absence of crystallographic data. On docking an Fe(III) atom into the structure of (PHPCP)H_2 (followed by CHARMm minimization), the phenolate oxygen moves 1.5 Å toward the porphyrin plane. This is accomplished by a screwing-down motion of the cap of the proposed structure of (PPCP)Fe^{III}. The free base, (PHPCP)H_2, has a ruffled structure of the porphyrin ring and a spiral shape of the capping legs, allowing a minimum exposure of the molecule to the solvent molecules. Upon Fe(III) ligation, the porphyrin ring flattens and brings more rigidity to the molecule. The greater flexibility of the free base is exhibited in composite motions of the capping structure (translation + rotation) about the z-axis and a ruffling behavior of the porphyrin ring. With increase in temperature, (PHPCP)H_2 gains in energy and undergoes structural changes. At low temperature (PHPCP)H_2 slows down its motion starting with the porphyrin ring and ending with the amide groups of the capping structure. There is a decrease in segmental mobilities of the legs C and D upon Fe(III) insertion.

Experimental Section

All NMR experiments were recorded at 500 MHz and 25° C in $CDCl_3$, unless otherwise specified. Chemical shifts were reported relative to the signal of $CHCl_3$ (^1H, 7.24 ppm; ^{13}C, 77.0 ppm) or $CDHCl_2$ (5.32 ppm). ^{13}C NMR of (PPCP)Fe^{III} was recorded with a t_{15} pulse of 3 μs, interpulse delay of 50 ms, and a spectral width of 142856 Hz. ^{13}C T_1 relaxation times were measured at 125.76 MHz by the standard inversion recovery

---

[18] Wüthrich, K. *NMR in Biological Research: Peptides and Proteins*; Elsevier: New York, 1976; p 73.

method.[19] ROESY spectra were collected using the Kessler pulse sequence:[1] $90°_x$-t_1-$(\beta_y$-$\tau)_n$-aquisition. Spectra were collected into 4K data blocks for 512 t_1 increments with a relaxation delay of 3 s, $\beta_y = 3\ \mu s$, $\tau = 24\ \mu s$, $n = 7491$ to give a mixing time of 200 ms with a locking field strength of 2.5 kHz and spectral width in both dimensions of 8333.33 Hz. Data matrix was zero-filled to 2 K and apodized with gaussian function to give a line broadening in both dimensions of 4 Hz. Quantitative data were obtained using eq 4, which includes also the offset correction,

$$r^6{}_{\mathrm{ab}} = K \sin^2(\beta_\mathrm{a}) \sin^2(\beta_\mathrm{b})/I_\mathrm{ab} \quad \beta_\mathrm{i} = \mathrm{arctg}(\gamma B_\mathrm{SL}/\omega_\mathrm{i}) \quad (4)$$

where r_{ab} is the distance between protons a and b, B_{SL} the field strength of the locking field,γ the magnetogyric ratio, ω_i the resonance offset of nucleus i, and K a constant evaluated from the cross peaks volume integral I_{ij} of proton i and j with known separation. For the ^{13}C–^1H chemical shift correlation, we used the pulse sequence and the workup described earlier.[1] For the Distance Geometry calculations, the porphyrin structures were built and minimized on a Silicon Graphics IRIS 4D/220 GTX workstation using the programs Quanta, version 3.3, and CHARMm, version 21.3 (Polygen Corp.).[2] The 12 distance constraints were 4 for E′–c {two distance constraints for both methylene protons and for each leg (C and D)}, 4 for E–ϵ {the same as for E′–c, but for legs A and B}, and 4 for 2,6–β {two distance constraints for both methylene protons of β to # 2 and # 6 proton}. The topology file PORPHYRIN.RTF was supplied by Polygen and the linkers were constructed in ChemNote, the 2D modeling facility in Quanta. Minimizations were performed in CHARMm until the energy change tolerance was less than 10^{-9} kcal/mol. Distance Geometry (DGEOM) program was supplied by E. I. du Pont de Nemours and uses an algorithm already reported.[20] The ROESY distance constraints were input using a constraints file, and the RMSFIT.MATRIX was cluster analyzed using a program Data Desk[10] (Odesta Corp.). The docking of Fe(III) into $(PHPCP)H_2$ was performed by inserting an Fe(III) atom at the midpoint of the four pyrrole nitrogens and minimizing the obtained structure with adopted basis Newton-Raphson (ABNR) parameters for 1000 steps until the energy differences were less than 10^{-9} kcal/mol. The helical turn was defined as the torsion of the cap {dihedral angle: A-center of the porphyrin ring-midpoint between 2′ and 6′-2′} divided by the distance (Å) between the center of the porphyrin ring and the midpoint between 2′ and 6′. The lateral shift was measured from the center of the porphyrin ring to the perpendicular from 1(1′) to the porphyrin plane. Molecular dynamics were performed in CHARMm using Verlet integration and the SHAKE algorithm to fix C–H bonds. Non bonded cutoffs and hydrogen bonding cutoffs were 14 and 5 Å, respectively.

Acknowledgment. This study was supported by a grant from the National Institutes of Health.

Supplementary Material Available: Table S1: CHARMm minimized energies for the 20 DGEOM representative structures. Table S2: ^1H chemical shifts of $(PHPCP)H_2$ between 5 and 55 °C. Figure S1: Expansion of the ^{13}C–^1H chemical shift correlation spectrum in the (110– 130) ×(5.5–8.0) ppm region. Figure S2: Expansion of the ^{13}C–^1H chemical shift correlation spectrum in the (20–37) × (–0.6–2.9) ppm region. The coordinate files (.CRD) of $(PHPCP)H_2$ and $(PPCP)Fe^{III}$ (13 pages). This material is contained in libraries on microfiche, immediately follows this article in the microfilm version of the journal, and can be ordered from the ACS; see any current masthead page for ordering information.

---

[19] (a) Cutnell, J. D.; Bleich, H. E.; Glasel, J. A. *J. Magn. Reson.* **1976**, *21*, 43. (b) Freeman, R.; Kempsell, S. P.; Levitt, M. H. *J. Magn. Reson.* **1980**, *38*, 453.

[20] (a) Crippen, G. M. *Distance Geometry and Conformational Calculations*; Bawden, D., Ed.; Research Studies Press, John Wiley: New York, 1981. (b) Havel, T. F.; Kunoto, I. D.; Crippen, G. M. *Bull. Math. Biol.* **1983**, *45*, 665.